Thermal Activation of a Group II Intron Ribozyme Reveals Multiple Conformational States†

James S. Franzen, Mincheng Zhang, Teresa R. Chay, and Craig L. Peebles*

Department of Biological Sciences, University of Pittsburgh, Pittsburgh, Pennsylvania 15260

Received April 21, 1994; Revised Manuscript Received July 1, 1994®

ABSTRACT: Conformational changes often accompany biological catalysis. Group II introns promote a variety of reactions *in vitro* that show an unusually sharp temperature dependence. This suggests that the chemical steps are accompanied by the conversion of a folded-but-inactive form to a differently folded active state. We report here the kinetic analysis of 5′-splice-junction hydrolysis (SJH) by E1:12345, a transcript containing the 5′-exon plus the first five of six intron secondary structure domains. The pseudo-first-order SJH reaction shows (1) activation by added KCl to 1.5 M; (2) cooperative activation by added $MgCl_2$, n_{Hill} = 4.1–4.3, and $[MgCl_2]_{V_{max}/2} \approx 0.040$ M; and (3) a rather high apparent activation energy, $E_a \approx 50$ kcal mol^{-1}. In contrast, the 5′-terminal phosphodiester bond of a domain 5 transcript (GGD5) was hydrolyzed with $E_a \approx 30$ kcal mol^{-1} under SJH conditions; the 5′-GG leader dinucleotide presumably lacks secondary structure constraints. The effect of adding the chaotropic salt tetraethylammonium chloride (TEA) was also investigated. TEA reduced the melting temperatures of GGD5 and E1:12345. TEA also shifted the profile of rate *versus* temperature for SJH by E1:12345 toward lower temperatures without affecting the maximum rate. TEA had little effect on the rate of hydrolysis of the 5′-phosphodiester bond of GGD5. The high apparent activation enthalpy and entropy for SJH along with the effect of TEA on these parameters imply that conversion of an inactive form of E1:12345 to an active conformation accompanies enhanced occupation of the transition state as the temperature is raised to that for maximum SJH. Analytical modeling indicates that either a two-state model (open and disordered, with open being active) or a three-state model (compact, open, and disordered) could account for the temperature dependence of k_{SJH}. However, the three-state model is clearly preferable, since it does not require that the activation parameters for phosphodiester bond hydrolysis exhibit exceptional values or that the rates for the chemical steps of SJH respond directly to TEA addition.

Conformational changes are an important feature of many biological functions. For example, multiple conformational reactions are required during spliceosome assembly and the pre-mRNA splicing reactions (Moore et al., 1993). Group II introns perform two-step splicing reactions mechanistically similar to that of the nuclear spliceosome, proceeding through the same lariat intermediate. Group II introns are widespread in pre-mRNAs of fungal and plant mitochondria and chloroplasts (Michel et al., 1989), and examples have recently been described in eubacteria (Ferat & Michel, 1993). These introns are organized into six secondary structure domains (see Figure 1A) that must interact through a set of tertiary interactions to achieve their active structure (Michel et al., 1989). Efficient self-splicing of group II introns *in vitro* depends on adding high concentrations of magnesium plus monovalent-cation salts (Peebles et al., 1987). Additionally, the temperature optimum of self-splicing activity is substantially higher than the optimum growth temperatures of the source organisms [for example, see Peebles et al. (1986) and Kück et al. (1990)]. Although these *in vitro* requirements for specific ionic and thermal conditions are generally recognized [reviewed by Shub et al. (1994)], they have not been quantitatively assessed before. The addition of salts and the use of high reaction temperatures must substitute for the normal mitochondrial environment in achieving the pre-mRNA conformation capable of splicing. Thus, manipulating the *in vitro* reaction conditions serves to probe the active state of group II introns.

We focus here on a model reaction analogous to the first step of splicing, accurate 5′-splice junction hydrolysis (SJH;[1] see Figure 1B). The SJH reaction is especially active in KCl for transcripts from the yeast mitochondrial group II intron a5γ (Peebles et al., 1987; Jarrell et al., 1988). SJH has been kinetically analyzed using a *trans* reaction between E1:123, a transcript with the 5′-exon and the first three intron domains, and the essential intron domain, D5 (Franzen et al., 1993). In the current study, we have simplified the system by choosing E1:12345, a transcript containing D5 (Figure 1A). Use of E1:12345 effectively ensures a saturating concentration of D5. This transcript also simplifies the kinetic analysis by preventing other reactions of intact group II introns, such as branching and the second step of splicing, since D6 and the

† This work was financially supported in part by research grants from the National Science Foundation (MCB-9206525 to C.L.P. and DCM-8819245 to T.R.C.), by the Pennsylvania Affiliate of the American Heart Association (T.R.C.), and by intramural research funds from the University of Pittsburgh, including support for the purchase and operation of the Aviv 14DS UV–vis spectrophotometer and the AMBIS 4000 radioanalytic imaging system.

* To whom correspondence should be addressed. Phone: (412) 624-4648. Fax: (412) 624-4759.

® Abstract published in *Advance ACS Abstracts,* August 15, 1994.

[1] Abbreviations: E1:123, a transcript with the a5γ versions of the 5′-exon, E1, and the intron domains D1, D2, and D3; E1:12345, a transcript with the a5γ versions of E1 and domains D1, D2, D3, D4, and D5; 12′, a secondary cleavage product containing D1 and part of D2; ′2345, a secondary cleavage product containing part of D2, and all of D3, D4, and D5; GGD5, a transcript containing the 5′-leader sequence GG- followed by the 34-nucleotide sequence of the a5γ version of D5; EBS1, exon binding site-1; IBS1, intron binding site-1; ψ-IBS1, a 6/6 match to intron binding site-1 in D2; EDTA, ethylenediaminetetraacetic acid; nts, nucleotide units; HEPES, 4-(2-hydroxyethyl)-1-piperazineethanesulfonic acid; SDS, sodium dodecyl sulfate; SJH, splice junction hydrolysis; TEA, tetraethylammonium chloride.

0006-2960/94/0433-11315$04.50/0

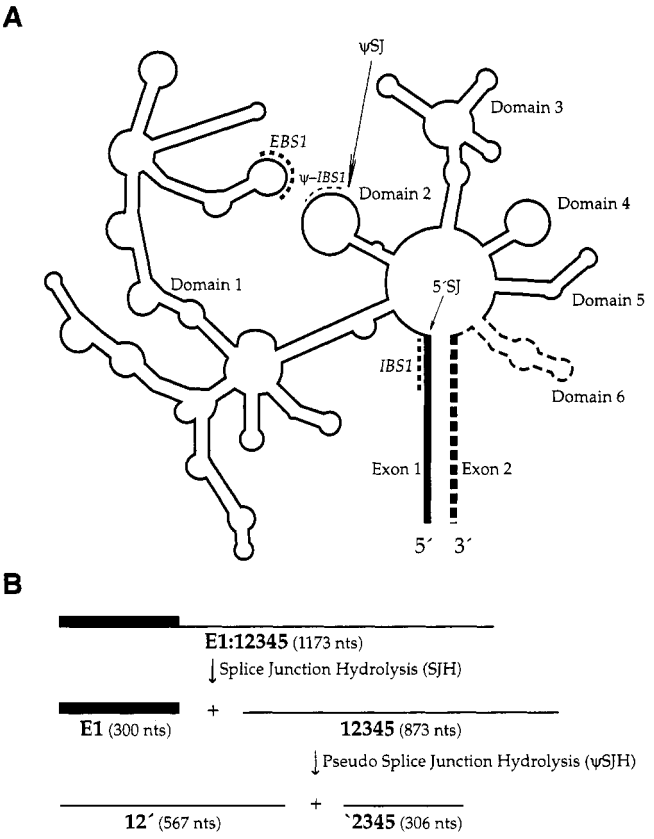

FIGURE 1: (A) Secondary structure of transcript E1:12345. The six secondary structure domains (Domain 1 through Domain 6) typical of a group II intron are drawn with a thin line; Exon 1 and Exon 2 are shown as straight heavy lines. Dashed-line regions (Domain 6 with its branch site, the 3'-splice junction, and Exon 2) are absent from E1:12345. Overbars mark sequences specifying cleavage sites (EBS1, exon binding site-1; IBS1, intron binding site-1; and ψ-IBS1, a six-out-of-six match to intron binding site-1 in Domain 2). Arrows indicate the locations of cleavage events. (B) Reaction pathway for SJH by transcript E1:12345. The principal products are diagrammed with their sizes indicated.

3'-splice junction are not included (Figure 1A). SJH by E1:12345 has been established as a pseudo-first-order reaction (Franzen et al., 1993); the products of SJH by E1:12345 and of a secondary cleavage by 12345 are diagrammed in Figure 1B.

Several processes involving RNA show a steep temperature dependence; such behavior has been interpreted as a signal of structural transition. For instance, renaturation of $tRNA_3^{Leu}$ is accompanied by an activation enthalpy of 69 kcal mol^{-1} and an activation entropy of 146 eu (Hawkins et al., 1977). Similarly, M1 RNA, the catalytic subunit of *Escherichia coli* RNase P, undergoes a transition to the active form with an Arrhenius activation energy of 36 kcal mol^{-1} (Altman & Guerrier-Takada, 1986). Likewise, the activation energy for transesterification between a tetranucleotide substrate and a denaturing-gel-purified circular group I intron ribozyme is about 50 kcal mol^{-1} (Sugimoto et al., 1988); however, this activation energy was reduced to 6 kcal mol^{-1} by controlled renaturation of the intron (Walstrum & Uhlenbeck, 1990). We report here that the activation energy for SJH by E1:12345 is nearly 50 kcal mol^{-1}. This suggests that group II introns as isolated *in vitro* depend on a conformational rearrangement for function in splicing and related reactions.

Further support for the occurrence of a structural transition along with SJH comes from the effect of adding TEA to SJH reactions. TEA is a classical water-structuring salt (Frank & Wen, 1957) that destabilizes protein structure (von Hippel & Schleich, 1969). TEA also has a dramatic chaotropic effect on DNA stability (Melchior & von Hippel, 1973; Schleich & Gould, 1974). Although TEA binds preferentially to A+T-rich regions of duplex DNA (Shapiro et al., 1969), TEA apparently interacts more effectively, albeit indiscriminately, with the nucleotide bases of single-stranded DNA (Melchior & von Hippel, 1973). We show in this study that the disrupting effect of TEA on protein and DNA secondary structure applies to RNA as well. We also show that there is a correlation between the action of TEA on RNA secondary structure and its effect on SJH activity. TEA significantly influences the temperature dependence of the rate of SJH by E1:12345, by reducing such activity at higher temperatures, but raising it at lower temperatures. On the other hand, TEA has virtually no effect on the activation parameters for the noncatalyzed cleavage of a phosphodiester bond unconstrained by secondary or tertiary structure interactions of its flanking nucleoside units. The observation that TEA shifts the profile of the SJH activity of E1:12345 along the temperature axis was closely examined. The deactivating effect at higher temperatures (due to RNA structure unfolding) and the activating effect at lower temperatures (also due to RNA structure unfolding) suggest that at least three intron conformational states exist. The characterization and interpretation of the TEA effects are presented here.

The observation of an exceptionally high activation energy for the SJH reaction and the effect of TEA on the rate of this reaction support our proposition that a conformational rearrangement occurs prior to the first chemical reaction of splicing by the isolated group II intron RNA.

MATERIALS AND METHODS

Preparation, Purification, and Preservation of RNA. GGD5 contains a two-nucleotide 5'-leader (GG-) plus the domain 5 sequence from intron a5γ of yeast mitochondrial DNA; GGD5 was transcribed from a synthetic DNA template by T7 RNA polymerase (Franzen et al., 1993; Milligan & Uhlenbeck, 1989). After alkaline phosphatase treatment, 5'-end-labeling was done with polynucleotide kinase and [γ-^{32}P]ATP. E1:12345 was transcribed from the *Hin*dIII-digested plasmid pJDI3'–851, obtained from P. S. Perlman (University of Texas, Dallas). Transcription was done at 37 °C for 30 min in the presence of [α-^{33}P]UTP. Each reaction mixture was applied directly to a denaturing polyacrylamide gel, and the desired transcript was separated, identified, excised, and electroeluted. After ethanol precipitation and vacuum drying, the RNA was dissolved in water. RNA concentrations were determined by spectrophotometry, using an average nucleotide molar extinction coefficient of 7500 M^{-1} cm^{-1} at 260 nm. Aliquots of freshly purified E1:12345 in water were dispensed into sterile silanized 0.2-mL MicroAmp PCR reaction tubes (Perkin-Elmer, Norwalk, CT) and dried in a Savant Speed-Vac concentrator at ambient temperature. The tubes of dry RNA were stored at −20 °C.

Splice Junction Hydrolysis. All SJH reactions were buffered with 0.02 M HEPES ($pH^{25°C}$ 7.1). The temperature and the concentrations of KCl, $MgCl_2$, TEA, and urea were varied as indicated for each experiment. If not explicitly stated otherwise, the standard concentrations of KCl and $MgCl_2$ were 0.50 and 0.060 M, respectively. Aqueous solutions of TEA (Aldrich, Milwaukee, WI) were decolorized with activated charcoal and filter sterilized. The TEA concentration of the resulting stock solution was determined by refractometry (Chang et al., 1974). For a given set of SJH rate measurements, 10-μL aliquots of the appropriate reaction buffers were added directly to the tubes with the dried E1:12345 and kept on ice. The initial concentration of

Scheme 1

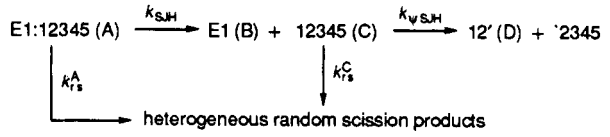

E1:12345 ranged from 2 to 30 nM, with most reactions at the upper end of this range. Reactions were initiated by transferring the tubes to the incubation bath. The thin-walled MicroAmp tubes allowed rapid thermal equilibration of the samples with the incubation bath. The apparent delay in product formation was less than 5 s, permitting reliable assay times as short as 1 min. The reactions were stopped by chilling and adding EDTA before analysis on 4% polyacrylamide gels containing 8 M urea. The gels were fixed, dried onto filter paper, scanned for radioactivity, and analyzed (Franzen et al., 1993). The progress of the SJH reaction is presented as the fraction of initially intact E1:12345 converted to E1 or 12345 (see Figure 1). This fraction was evaluated as the ratio of the net radioactivity in the E1 or 12345 bands (normalized to E1:12345-equivalent radioactivity) divided by the amount of full-length E1:12345 at the beginning of the reaction. The radioactivity histograms for the E1:12345-containing band of unreacted samples were always skewed toward the faster-migrating side, indicating the presence of some transcripts shorter than full-length. Shortened transcripts result from either premature transcription termination or random cleavage of full-length RNAs. Transcripts lacking sequences from their 5′-end yield short versions of E1, while transcripts lacking sequences from their 3′-end have lost D5 and are inactive. In either case, shortened transcripts do not contribute significantly to the relevant products. The amount of radioactivity in full-length transcript was defined as twice the amount of radioactivity in the E1:12345 half-peak behind its maximum for samples taken at zero time. Defined this way, the fraction of intact E1:12345 corresponded to 94% to 40% of the total RNA, with the degree of purity depending on how accurately the transcript was excised in preparation and on how long the sample had been stored.

According to the design of any particular experiment, the value of the rate constant for SJH (k_{SJH}) was determined by one of three methods.

Method i: Nonlinear regression fitting to eq 1 of the Appendix, which describes the reactions shown in Scheme 1.

Method ii: Linear fitting to the slopes of $[B]/[A]_0$ progress curves with five sampling times during the initial phase of the reaction. In the limit of short reaction times, eq 1 reduces to eq 1a of the Appendix.

Method iii: Direct calculation from single-time observations made within the empirically established time interval of linear E1 formation. Measurement of k_{SJH} by method iii was used to survey many reaction conditions using a single RNA preparation over a few days.

Nonspecific Cleavage of GGD5. Solutions of 5′-end-labeled GGD5 in standard reaction buffer (either with no additions, with TEA added to 1.0 M, or with KCl added to 1.5 M) were incubated as indicated at various temperatures to evaluate the kinetics of scission of the phosphodiester linkage at the 5′-end of the molecule. These reaction products were separated on 20% polyacrylamide gels with 8 M urea.

Thermal Denaturation Profiles. Melting curves were obtained with the Aviv 14DS UV–vis Spectrophotometer using the thermoelectric temperature-regulated cell holder. The RNA solutions had net A_{260} values between 0.45 and 1.0 at 0 °C. The cuvette jacket temperature was raised from 0 to 75 °C for melting E1:12345 and from 0 to 100 °C for melting GGD5. A heating rate of 2 °C min^{-1} was used for all of the meltings reported. The melting profile of GGD5 at a heating rate of 2 °C min^{-1} was not distinguishable from profiles measured at 1 or at 4 °C min^{-1}. After 3 min at the temperature maximum, the sample was cooled to 0 °C at the same rate. The values of A_{260} were recorded at time intervals corresponding to 0.5 °C changes throughout the entire cycle of heating and cooling. The cuvette temperature was calibrated using optical thermometry. The calibration function was obtained by measuring the values of $[(A_{T°C} - A_{0°C})/A_{0°C}]_\lambda$ at 255 nm over a series of equilibrated jacket temperatures from 0 to 90 °C with a 0.050 M EDTA solution. EDTA has a strongly temperature dependent UV absorbance. The quantity $[\Delta A_{T°C}/A_{0°C}]_\lambda$ is independent of the concentration of the chromophore chosen for the thermometer. The resulting optical thermometer function was used to evaluate the cuvette temperature during controlled heating and cooling of EDTA solutions, allowing the construction of cuvette temperature *versus* jacket temperature calibration relations for each heating and cooling program. The absorbance *versus* temperature profile for each buffer was measured, and these profiles served as baselines to evaluate the net hyperchromic shift due to nucleic acid structural change. Melting of GGD5 was done both with 0.02 M HEPES and with 0.02 M cacodylate to assess the possible influence of temperature-dependent pH changes on the thermal stability of the nucleic acid. All RNA meltings done in the presence of 0.0005 M EDTA were fully reversible.

Determination of Parameter Values from Experimental Data. Kinetic rate constants were evaluated by nonlinear regression fitting to the appropriate progress function for product formation (see section A of the Appendix). Fitting was achieved by using the DeltaGraph software application (DeltaPoint, Inc.), which uses the Levenberg–Marquardt algorithm. The thermodynamic parameters appearing in eqs 6a and 7a were also evaluated by nonlinear least squares fitting. Minimization of the sum of the squares of the deviates between the experimental points and the theoretical curve was performed with the subroutine ZXMWD in the IMSL (International Mathematical Statistical Library) software package. For eq 7a, minimization was done without any constraint on the parameters. For eq 6a, however, the value of the activation entropy, $\Delta S^\ddagger$, was set equal to 0. The value of the activation enthalpy, $\Delta H^\ddagger$, thus obtained for the TEA-absent data and the imposed value of $\Delta S^\ddagger$ (=0) were applied to the analyses by eq 6a of the sets of TEA-present data. Minimizations of the TEA-absent data according to eq 6a were also performed with fixed $\Delta S^\ddagger$ values of −10 eu and 10 eu, yielding final values for the sum of the squares of the deviates analogous to that obtained using $\Delta S^\ddagger = 0$. However, application of either of these non-zero $\Delta S^\ddagger$ values, along with its companion $\Delta H^\ddagger$ value, to the analysis of the temperature dependence of k_{SJH} in the presence of TEA increased the final sums of the squares of the deviates severalfold.

RESULTS AND DISCUSSION

The principal products of SJH by E1:12345 are E1 (300 nts) and 12345 (873 nts) (Figure 1A); initially these products are equimolar even though E1:12345 is simultaneously consumed by a parallel process of random scission (Figure 2). Evaluation of the rate constants for SJH and random scission required knowledge of the amount of E1:12345 present at the start of the reaction. Although measuring the yield of E1 accumulated by late reaction times might have served as an estimate of the amount of E1:12345 present at time zero, such an estimate would be valid only if k_{rs}^{A} were negligible relative

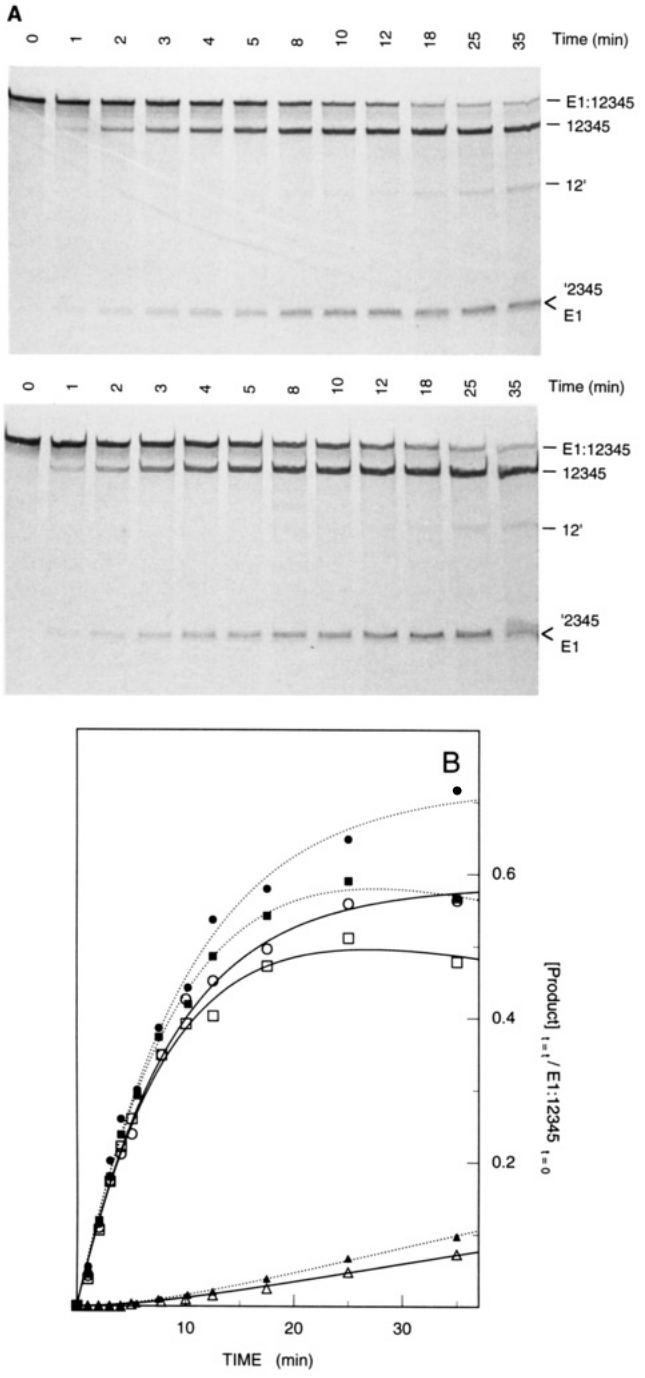

FIGURE 2: (A) Products of SJH by E1:12345. Upper panel: The reactions were performed at 48 °C in 0.50 M KCl, 0.060 M $MgCl_2$, and 0.020 M HEPES, pH 7.1. The products were separated on a 4% polyacrylamide gel with 8 M urea. Lower panel: The reactions were performed as for the upper panel, but at 44 °C and with 0.5 M TEA. (B) Progress curves for SJH product formation. Reduced data are shown for the experiments of panel A: f_{E1}, circles; f_{12345}, squares; $f_{12'}$, triangles; solid lines and open symbols, non-TEA-containing samples; dotted lines and closed symbols, 0.50 M TEA-containing samples. The quantities of each product were determined from AMBIS radioanalytic images with appropriate background correction (Franzen et al., 1993). The curves are drawn as nonlinear regression fits to the data using eqs 1, 2, and 3 of the Appendix. The values for E1 after the time of 12′ appearance (≈10 min) were corrected for the presence of ′2345 (306 nts) which migrated with E1 (300 nts). The governing rate constants were found and are listed here.

rate constant (min^{-1})	0.0 M TEA$^{48°C}$	0.5 M TEA$^{44°C}$
k_{SJH}	0.067	0.072
k_{rs}^{A}	0.047	0.026
$k_{\psi SJH}^{C}$	0.0051	0.0061
k_{rs}^{C}	0.0012	0.0019

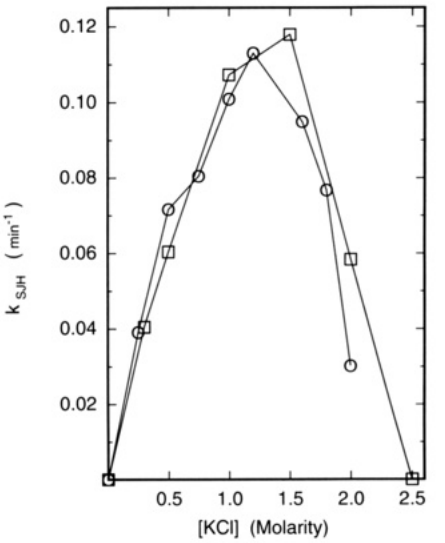

FIGURE 3: Effect of KCl on the SJH reaction rate. The reactions were performed for 3 min at 48 °C. Circles and squares represent different transcript preparations.

to k_{SJH}. Using our empirical estimate of the initial amount of E1:12345, we found that the loss of reactant by random scission was too great to neglect. Since experimental uncertainty in the initial amount of E1:12345 always introduces uncertainty into k_{SJH} directly, it was advantageous to incorporate an index of reactant purity in the analysis.

The delayed formation of intron fragment 12′ (567 nts) clearly indicates that this cleavage at a pseudo-5′-splice junction in D2 follows rather than parallels *bona fide* SJH (Figure 1B; Jarrell et al., 1988; Franzen et al., 1993). Nonspecific cleavage of E1:12345 and 12345 also reduces the actual accumulation of E1 and 12′. If nonspecific cleavage were negligible ($k_{rs}^{A} \sim 0$), the observed initial rate of E1 formation would lead to about 90% conversion of the E1:12345 to E1 plus 12345 after 35 min. Similarly, if 12345 were cleaved only at the secondary site ($k_{rs}^{C} \sim 0$), the sum of 12345 plus 12′ would equal the yield of E1. The values of the rate constants for this system modeled according to Scheme 1 are shown in the caption of Figure 2. The rate constant values for any given set of conditions were independent of the initial concentration of E1:12345. The sequential nature of splice junction and secondary site cleavages suggests that the initial product is the binary complex E1·12345 that then dissociates to give E1 and 12345. Subsequently, 12345 must change conformation to allow EBS1 to interact with the pseudo-IBS1 in D2 (Figure 1A). This rearrangement is presumably necessary to activate the secondary cleavage. The delayed appearance of 12′ apparently reflects either the slow release of E1, a slow conformational change by 12345, or intrinsically slow hydrolysis of the secondary cleavage site after rapid E1 release and rapid refolding. The absence of a visible band for the companion fragment ′2345 is due to the migration of ′2345 (306 nts) with E1 (300 nts). In a separate experiment, the 12345 and E1 products of SJH by E1:12345 were isolated by gel electrophoresis and subjected to SJH conditions. 12345 directly produced 12′ and ′2345; notably, ′2345 migrated with E1 produced by SJH from E1:12345 (data not shown).

There is a well-known *in vitro* requirement for added electrolytes in the promotion of efficient group II intron reactions (Peebles et al., 1987; Kück et al., 1990; Koch et al., 1992). Figure 3 presents the response of SJH by E1:12345 to added KCl. Although optimal activity is achieved near 1.5 M KCl, we chose 0.50 M KCl as the standard condition because

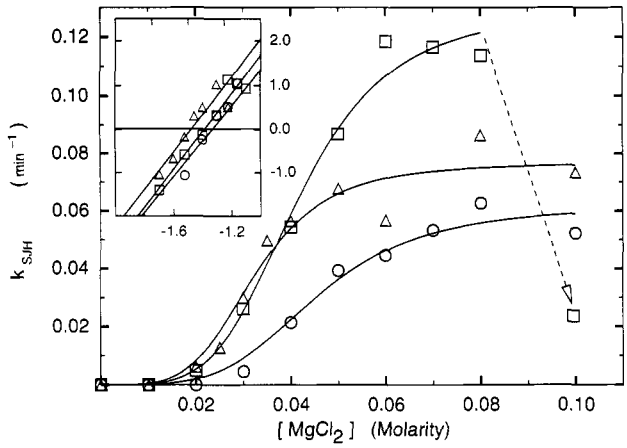

FIGURE 4: Effect of $MgCl_2$ on the SJH reaction rate. Conditions for the three reaction sets were as follows: (○) 48 °C, 0.50 M KCl; (□) 48 °C, 1.0 M KCl; (△) 42.5 °C, 0.50 M KCl + 0.50 M TEA. The rate constants were determined by method iii. The reaction times varied, but all were within the linear period of product formation. The curves are Hill functions, $k_{SJH} = k_{SJHmax}\cdot[MgCl_2]^n/(([MgCl_2]_{0.5v_{max}})^n + [MgCl_2]^n)$, developed by using the parameters obtained from the inset Hill plots of log $k_{SJH}/(k_{SJHmax} - k_{SJH})$ *versus* log $[MgCl_2]$. The characteristic values of n_{Hill}, $[MgCl_2]_{0.5}$, and k_{SJHmax} were as follows: (○) 4.1, 0.046 M, and 0.062 min^{-1}; (□) 4.3, 0.042 M, and 0.129 min^{-1}; and (△) 4.3, 0.033 M, and 0.077 min^{-1}.

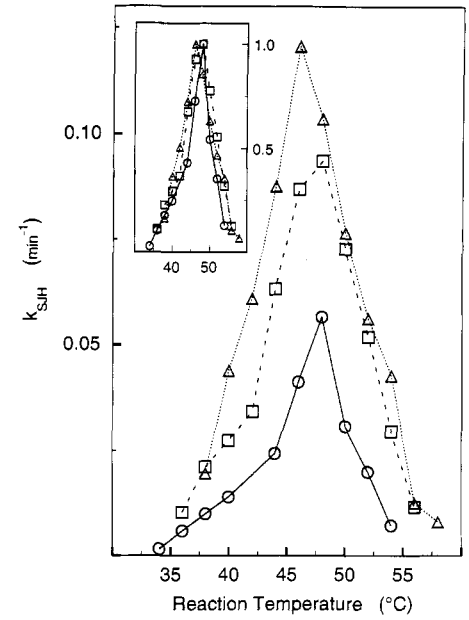

FIGURE 5: Effect of temperature on the SJH reaction rate at different KCl concentrations. The rate constants were determined by method iii and are shown for three conditions: (○) 0.50 M KCl, (□) 1.0 M KCl, and (△) 1.5 M KCl. The inset shows the data normalized to the rate at the temperature optimum for each KCl concentration.

of our plan to test the effect of adding another electrolyte, TEA. Since KCl concentrations above 1.5 M diminished SJH activity, it seemed judicious not to exceed a total monovalent salt concentration of 1.5 M.

The response of SJH by E1:12345 to added $MgCl_2$ demonstrates that the action of Mg^{2+} is cooperative for group II introns (Figure 4). We have found essentially the same cooperative effect of $MgCl_2$ for SJH in the *trans* system of E1:123 plus D5 (data not shown). Thus the cooperative effect of Mg^{2+} on SJH is not peculiar to any specific transcript. In 0.50 M KCl, $MgCl_2$ above 0.14 M led to a significant decline of activity (data not shown), while $MgCl_2$ above 0.08 M inhibited SJH in 1.0 M KCl (Figure 4). The Hill coefficients (see the inset diagram of Figure 4) indicate that induction of activity is accompanied by binding of at least four Mg^{2+} ions. The cooperative interaction of four or more Mg^{2+} ions with E1:12345 implies that Mg^{2+} binding allows the RNA to assume an active state. This is reminiscent of other ribozyme systems, where cooperative binding of Mg^{2+} has a role in organizing the structure. For example, folding of the group I intron from the rRNA gene of *Tetrahymena thermophila* (as measured by its sensitivity to Fe^{2+}-EDTA cleavage) responds cooperatively to $MgCl_2$, with $n_{Hill} = 2.7$ and $[MgCl_2]_{0.5} = 1$ mM (Celander & Cech, 1991). The endonuclease activity of the same ribozyme in the presence of 1 mM $CaCl_2$ displayed a cooperative response centered at about 0.5 mM $MgCl_2$ (Grosshans & Cech, 1989). The activity of *Bacillus subtilis* RNase P RNA also showed a cooperative response to $MgCl_2$, with $n_{Hill} \approx 3$ and $[MgCl_2]_{0.5} \approx 10$–50 mM (Smith & Pace, 1993). The relatively high salt requirement for RNase P activity resembles that of group II introns. We have no basis at this time to decide whether any of the activity-inducing Mg^{2+} ions are positioned directly in the active site of group II introns or instead participate at a distance from the catalytic center to mold an active conformation. If direct catalytic action occurs, one (or more) of the Mg^{2+} ions may assist the departure of the leaving group in the transition state, as has been demonstrated for the group I ribozyme (Piccirilli et al., 1993). Alternatively (or in addition), Mg^{2+} might facilitate hydroxide ion attack, as proposed for RNase P (Smith & Pace, 1993) and for pre-mRNA spliceosomes and group II introns (Steitz & Steitz, 1993). Regardless of the mode of action, the cooperative activation by Mg^{2+} implies that the association of a set of Mg^{2+} ions with E1:12345 is needed to achieve the active state. For the remaining experiments of this investigation, 0.50 M KCl, 0.060 M $MgCl_2$, and 0.020 M HEPES, pH 7.1, was selected as the reference reaction buffer. By this choice, the total concentration of monovalent cation salts never exceeded 1.5 M, even with TEA added to concentrations as high as 1.0 M.

Although adding TEA affected the temperature optimum for SJH (see below), adding TEA had little effect on the concentration range for activation by $MgCl_2$, the magnitude of the effect, or the cooperativity of the process. In a separate experiment, the addition of $MgCl_2$ to the transcript E1:123 was observed to induce significant *hypo*chromism (data not shown). This saturable *hypo*chromic effect was followed at 45 °C, the temperature for maximum SJH of the *trans* system E1:123 + GGD5 (Franzen et al., 1993); the response was not sigmoidal with half-saturation occurring at 10 mM $MgCl_2$. This result provides evidence for the general binding of Mg^{2+} ions to the group II intron RNA. The total number of Mg^{2+} ions bound to E1:12345 at 0.060 M $MgCl_2$ is not known, but the cooperatively bound Mg^{2+} ions allow E1:12345 to achieve the proper conformation for SJH, either with KCl alone or with KCl plus TEA.

The temperature dependence of SJH by E1:12345 in 0.50 M KCl (Figure 5) is almost the same as that of the *trans* SJH reaction between E1:123 and GGD5 (Franzen et al., 1993) and resembles the response of self-splicing by the intact intron (Peebles et al., 1986). Raising the KCl concentration to 1.0 or 1.5 M increased the reaction rate throughout the temperature range (Figure 5), as expected from the data of Figure 3. However, changing the KCl concentration had little effect on T_{max}, the temperature of maximum k_{SJH} (T_{max} = 48 °C for 0.50 M KCl *versus* 46 °C for 1.5 M KCl), or the shape of the temperature response (Figure 5, inset).

The temperature dependence of SJH was also examined using method ii to determine the value of k_{SJH} more precisely (Figure 6A). These results verify the strong activating effect of increasing the temperature to 48 °C in 0.50 M KCl (Figure 6B, open circles). The decrease in k_{SJH} at still higher

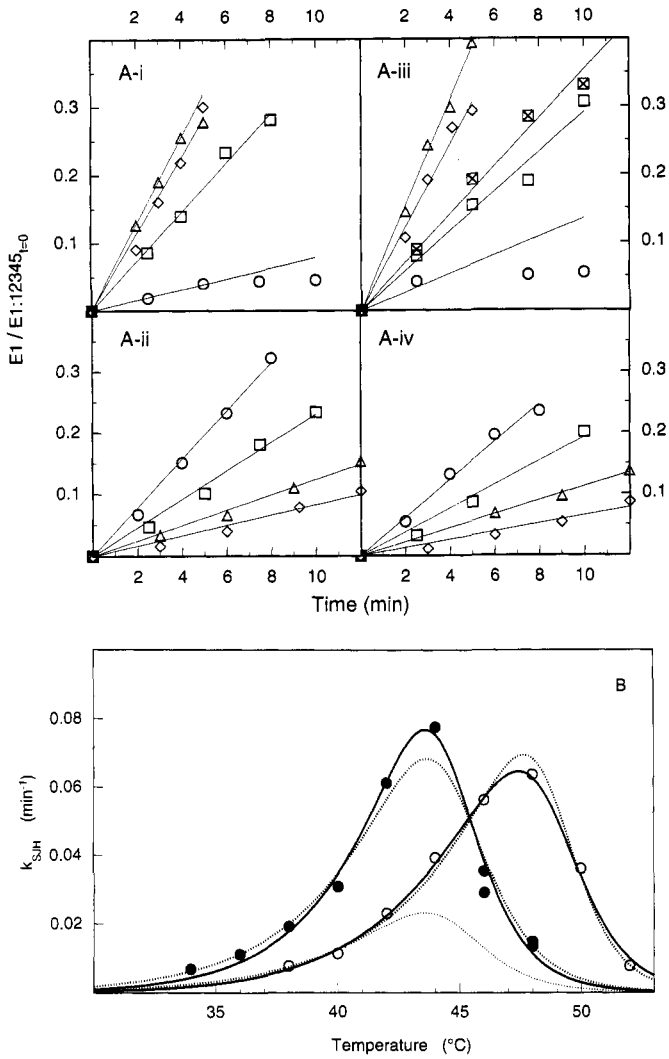

FIGURE 6: Effect of TEA on the temperature variation of the SJH rate. (A) E1 formation curves: panels i and ii, no TEA present; panels iii and iv, 0.50 M TEA. Temperatures were as follows. Panel i: 52, ○; 50, □; 48, △; 46 °C, ◇. Panel ii: 44, ○; 42, □; 40, △; 38 °C, ◇. Panel iii: 48, ○; 46, □; 44, △; 42 °C, ◇. Panel iv: 40, ○; 38, □; 36, △; 34 °C, ◇. (B) Observed and theoretical temperature dependence of k_{SJH}: open circles, no TEA present; closed circles, 0.50 M TEA. The heavier dashed lines represent fitting according to the two-state model (Appendix eq 7a); the lighter dashed line represents attempted two-state fitting of the 0.50 M TEA data using the apparent $\Delta H^{\ddagger}$ and $\Delta S^{\ddagger}$ values obtained by fitting the 0.0 M TEA data by the two-state model. The solid lines represent fitting according to the three-state model (Appendix eq 6a). See Table 3 for the parameter values from these fittings.

temperatures is probably due to the disruption of some RNA structure essential for SJH activity. Melting and annealing of denaturing-gel-purified group I ribozyme preparations considerably alters the temperature responsiveness of ribozyme activity (Walstrum & Uhlenbeck, 1990). To learn whether the observed temperature dependence of k_{SJH} was due to some metastable RNA structure induced by denaturing gel purification, SJH rates were also measured with RNA samples preheated at 95 °C for 1 min in the standard buffer without $MgCl_2$ but with 0.0005 M EDTA. After the samples were cooled and $MgCl_2$ was added to 0.060 M, SJH was assayed over the temperature range spanned by Figure 6B. This preheating and annealing treatment yielded results not significantly different from the same experiment without preheating (open circles, Figure 6B). We analyzed the data of Figure 6B in terms of a two-state system composed of SJH-active and -inactive forms (see eq 7a of the Appendix). With this two-state model, the numerator of the expression for k_{SJH} depends on the apparent activation enthalpy and entropy of the SJH reaction, $\Delta H^{\ddagger}$ and $\Delta S^{\ddagger}$. The dashed line with a maximum at 48 °C represents fitting to the two-state model and yields $\Delta H^{\ddagger}$ and $\Delta S^{\ddagger}$ of 50 kcal mol^{-1} and 86 eu, respectively.

The activating effect of temperature on SJH is exceptionally large below T_{max}; the $\Delta S^{\ddagger}$ value is also surprisingly large. Together, these parameter values imply that an input of heat energy is needed both for an RNA conformational change and for increasing the population of the transition state. To test this expectation, we examined the kinetics of phosphodiester bond breakage in a context where cleavage chemistry is not complicated by secondary and tertiary structure constraints. The 5′-leader (GG-) dinucleotide of GGD5 RNA was chosen as our model reactant because it is probably freely mobile and because we could readily prepare 5′-end-labeled GGD5 from materials on hand. GGD5 is sensitive to the same process of random scission as larger transcripts such as E1:123 (Franzen et al., 1993) and E1:12345. Although this kind of scission is probably initiated by attack of the 2′-OH adjacent to the 3′–5′ phosphodiester linkage, and thus differs from attack by water in SJH, it is nevertheless likely to proceed through a pentacovalent phosphorus transition state. Therefore, hydrolysis of the terminal nucleotide of GGD5 serves as a model for obtaining the intrinsic activation energy for phosphodiester bond cleavage under the solvent conditions used in this study. Following the general treatment of random scission (Simha, 1941; Tanford, 1961) with modification for an end-labeled polymer, it can readily be shown that formation of labeled monomer obeys the simple first-order reaction progress curve, $P = A_0(1 - e^{-kt})$. The labeled monomer product *pGp results from cleavage of the phosphodiester bond at the 5′-end of the initial reactant or of any radioactive intermediate, and the statistical weight for generating this monomer is always unity. Progress curves for *pGp appearance under various salt conditions and at different temperatures show that these spontaneous cleavage reactions are relatively slow (Figure 7). As expected, the activation parameters hardly change with solvent composition, and the temperature dependence of the rate is much smaller than for SJH of E1:12345, with $\Delta H^{\ddagger}_{pGpG\sim\ cleavage} \approx 30$ kcal mol^{-1} and $\Delta S^{\ddagger}_{pGpG\sim\ cleavage} \approx -1$ to $+13$ eu (Table 1). The rate constant for SJH by E1:12345 under our standard conditions is about 0.07 min^{-1} (Figures 2B, 3, 4, 5, 6B, and 8). This value is an order of magnitude less than the rate constant for hydrolysis of a 5′-splice junction substrate by a group I ribozyme in 0.050 M buffer at pH 6.7 with 0.010 M $MgCl_2$ at 50 °C (Herschlag & Cech, 1990). The group II rate constant is three orders of magnitude less than the rate constant for the hydrolytic cleavage of pre-tRNA catalyzed by RNase P in 1.0 M NaCl and 25 mM $MgCl_2$ at 37 °C (Smith & Pace, 1993). A lower limit for the rate enhancement of phosphodiester bond cleavage by the group II intron structure may be estimated by comparing the SJH rate for E1:12345 with the rate of 5′-terminal nucleotide cleavage of GGD5. At 48 °C under our standard conditions, the rate constant for the 5′-terminal nucleotide cleavage of GGD5 was calculated from the data of Table 1 to be 2.6×10^{-5} min^{-1}. The 2600-fold larger rate constant for SJH indicates the effect achieved by group II intron folding; this folding results in the proper alignment of the structural elements that promote enhanced reactivity at the 5′-splice junction. The effect might be even larger, since the mechanism of terminal nucleotide hydrolysis from GGD5 probably involves initial attack by a vicinal 2′-OH group, while SJH probably proceeds by direct attack of water (Jarrell et al., 1988).

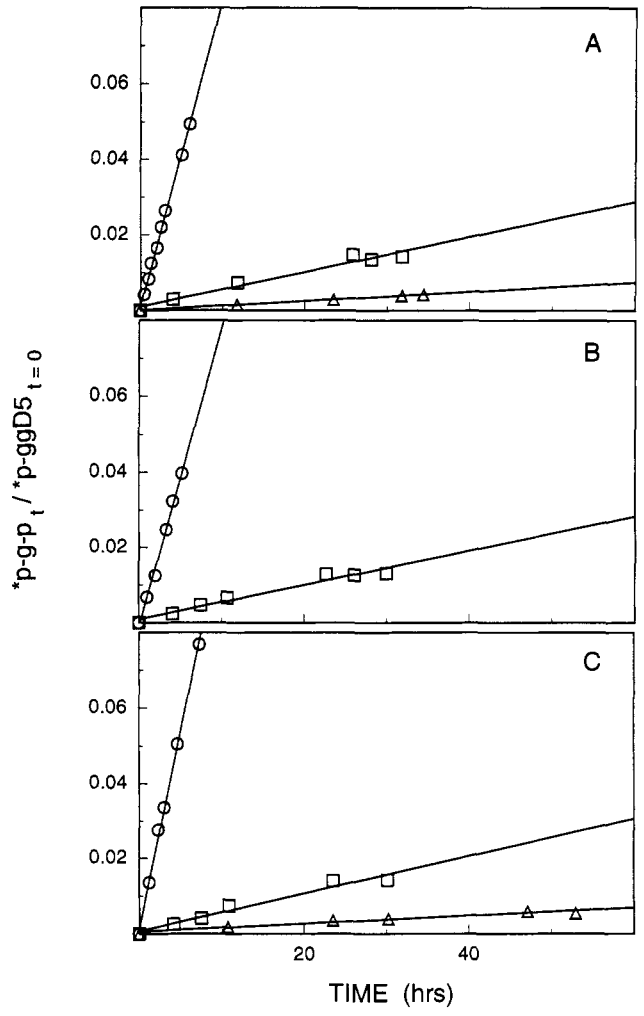

FIGURE 7: Effect of temperature on the rate of 5′-terminal phosphodiester bond cleavage of GGD5. (A) 0.50 M KCl. (B) 0.50 M KCl + 1.0 M TEA. (C) 1.5 M KCl. The reaction temperatures were (○) 60, (□) 42, and (△) 30 °C.

Several observations about the 5′-terminal nucleotide cleavage of GGD5 are of particular significance. First, this hydrolysis reaction showed the same sensitivity to temperature as the hydrolysis of either dimethyl or monomethyl phosphate (see the $\Delta H^{\ddagger}$ values of Table 1). Second, the 5′-terminal nucleotide cleavage of GGD5 was insensitive to TEA addition. Third, the $\Delta S^{\ddagger}$ value for this reaction is in the range of values obtained for hydrolysis of the small-molecule alkyl phosphates. These findings show that the terminal cleavage of GGD5 is not extraordinary with respect to thermal activation. Therefore, at least with respect to thermal effects, it is probably a reasonable model for intrinsic hydrolysis at the 5′-splice junction. The lack of an effect of TEA on the hydrolysis of the 5′-terminal nucleotide of GGD5 thus suggests that the chemical step of SJH *per se* is not especially sensitive to TEA addition.

Although TEA appears not to influence the kinetics of *pGp release from GGD5 (Figure 7 and Table 1), it does significantly shift the temperature dependence of SJH by E1:12345 (Figure 6B, compare open and solid circle data). Notably, TEA does not change the reaction pathway, since the same products appeared at nearly the same rates in 0.50 M KCl plus 0.50 M TEA at 44 °C as in 0.50 M KCl at 48 °C (Figures 2A (lower panel), 2B, and 6B). The 0.50 M TEA data of Figure 6B can be fit with a two-state (SJH-active and disordered) model, but this requires increasing the $\Delta H^{\ddagger}$ and $\Delta S^{\ddagger}$ values by 3.6 kcal mol^{-1} and 13 eu, respectively (Table 3 and section B of the Appendix). The shift of T_{max} in response to TEA addition would be primarily due to the disordering effect of TEA on RNA structure; for this two-state formulation of the system, T_{OD} (the midpoint temperature of the transition to the disordered state) decreased from 48.8 to 44.6 °C.

The SJH activity *versus* temperature profile shifted to successively lower temperatures with progressive addition of TEA to 1.0 M. In 0.50 M KCl, T_{max} declined from 49 to 40 °C as the TEA concentration increased from 0.0 to 1.0 M (Figure 8A). Up to 0.80 M, TEA had only a small effect on the magnitude of SJH activity at T_{max}. However, SJH was not detectable when 1.25 M TEA was added or when KCl was completely replaced by TEA (data not shown). In 1.0 M KCl, the value of T_{max} was again lowered as TEA was progressively added, but there was also a pronounced decline in activity at T_{max} (Figure 8B). We also tested the response to added urea, a denaturant which had a distinct effect on the temperature response of SJH (Figure 8C). In 0.50 M KCl plus 0.50 M urea, T_{max} was shifted to 44 °C, but the activity at T_{max} was only half of that observed in 0.50 M KCl plus 0.50 M TEA. Adding urea to 1.0 M did not change the temperature profile further, while no SJH was detected at any temperature when 1.5 M urea was added.

The effects of temperature and TEA might be attributed to pH changes trivially affecting the SJH rate. Such a pH effect might be due to acidic or basic contaminants of the TEA stock solution or to the temperature dependence of the buffer pK_a. Adding 0.50 or 1.0 M TEA to mixtures containing 0.50 M KCl, 0.060 M $MgCl_2$, and either 0.020 or 0.040 M HEPES (apparent pH$^{25°C}$ = 7.3) or cacodylate (apparent pH$^{25°C}$ = 6.7) did not change the pH beyond experimental error. The variation of pH with temperature from 25 to 50 °C in 0.50 M KCl plus 0.060 M $MgCl_2$ was –0.023 ± 0.006 deg^{-1} for HEPES buffer and –0.003 ± 0.003 deg^{-1} for cacodylate buffer. The observed changes of SJH rate with temperature are much too large to be attributed to the small pH variations that characterize these solvent systems. Also, considering the rate-enhancing effect of increased pH on self-splicing promoted by the a5γ intron (Peebles et al., 1987), the negative pH temperature coefficient of HEPES buffer would only serve to reduce, not increase, any apparent activating effect of temperature on k_{SJH}.

The effect of TEA on RNA structure was measured as the heat-induced UV hyperchromicity of GGD5 and E1:12345. Under SJH reaction conditions, both GGD5 and E1:12345 are susceptible to increasing random scission as the temperature is raised, while E1:12345 undergoes SJH as well. Therefore, these RNAs were melted without added $MgCl_2$ and with 0.0005 M EDTA present to chelate residual Mg^{2+}. While adding KCl raised the T_m of GGD5, adding TEA reduced the T_m (Figure 9 and Table 2). The parameters for melting (Table 2) were evaluated according to the conventional two-state model (Petersheim & Turner, 1983). After the heating and cooling cycle, the GGD5 showed no sign of degradation and remained fully active for SJH in *trans*. TEA also lowered the apparent T_m of E1:12345 from 49 to 37.5 °C as the TEA concentration was increased to 1.0 M (Figure 10A). On the basis of charge shielding alone, TEA was expected to stabilize RNA structure, but the structure-disrupting influence of TEA predominated. At least in the presence of 0.50 M KCl, the RNA-melting effect of TEA appears to be entropic (Table 2). Melting E1:12345 in 0.50 M urea revealed very little effect on the apparent T_m, although the transition was broadened (data not shown).

E1:12345 was also melted with 0.060 M $MgCl_2$ present (Figure 10B). The addition of Mg^{2+} at a concentration sufficient to support SJH considerably stabilized the RNA

Table 1: Rate Constants and Activation Parameters for the 5′-Terminal Nucleotide Cleavage from GGD5 and for the Hydrolysis of Other Selected Phosphate Esters

reactants	condition	temp (°C)	$10^6 \times k_{rate}$ (min^{-1})	$\Delta H^{\ddagger}$ (kcal mol^{-1})	$\Delta S^{\ddagger}$ (eu)	ref.
GGD5 + H_2O	pH 7.1	30	2.1			
	0.50 M KCl	42	7.8	28 ± 1	−1 ± 4	this work
	0.06 M $MgCl_2$	60	136			
	pH 7.1					
	0.50 M KCl	42	7.6	32 ± 1[a]	11 ± 4[a]	this work
	1.0 M TEA	60	132			
	0.06 M $MgCl_2$					
	pH 7.1	30	1.8			
	1.5 M KCl	42	8.3	30 ± 3	7 ± 9	this work
	0.06 M $MgCl_2$	60	175			
$(CH_3O)_2PO_2^-$ + OH^-	pH 13			28.2[b]	−12[b]	Kumomoto et al. (1956)
	m = 1.1					
$(CH_3O)_2OPOH$ + H_2O	pH 1.24			25.5[b]	−15[b]	Bunton et al. (1960)
	0.05 M KCl					
$(CH_3O)OPO_2^-$ + H_2O	pH 4.1			30.6	0.1	Bunton et al. (1958)
(2-hydroxypropyl)methyl phosphate	0.05 N NaOH			16.2	−30	Brown and Usher (1965)

[a] Error estimated by propagation-of-error analysis. [b] Calculated from reported E_a and preexponential factor values.

Table 2: KCl and TEA Effects on the Parameters for GGD5 Melting[a]

[TEA] (M)	parameter	0.0 M KCl	0.50 M KCl	1.0 M KCl
0.0	T_m (°C)	59.3	77.9	79.8
	$\Delta H°$ (kcal mol^{-1})	68.1	56.3	53.7
	$\Delta S°$ (eu)	205	161	152
0.5	T_m (°C)	29.4	66.6	
	$\Delta H°$ (kcal mol^{-1})	54.2	59.1	
	$\Delta S°$ (eu)	168	174	
1.0	T_m (°C)	44.5		
	$\Delta H°$ (kcal mol^{-1})	54.4		
	$\Delta S°$ (eu)	171		

[a] The tabulated parameter values were obtained by fitting according to a two-state model (Petersheim & Turner, 1983). In all cases the solutions being melted contained 0.02 M cacodylate buffer, pH 7.0, and 0.0005 M EDTA.

against melting. Nevertheless, significant hyperchromicity developed by 48 °C, the temperature optimum for SJH. The apparent relative *hypo*chromicity at high temperature was unexpected, but this effect was observed consistently and was time-dependent, settling to a limiting value of about 27% on the hyperchromicity axis. Subsequent cooling generated an annealing curve quite different from the melting curve. Clearly, the melting and annealing cycle performed in 0.060 M $MgCl_2$ was not reversible. This same cycle in the absence of Mg^{2+} had virtually no effect on the integrity and SJH activity of E1:12345 (Figure 10B, inset traces a, b, and c). When the experiment was done in 0.060 M $MgCl_2$, some E1 was produced during melting to 75 °C; there was also considerable transcript degradation (Figure 10B, inset trace d) as well as complete loss of SJH activity for the residual intact transcript (Figure 10B, inset trace e relative to d). Whether or not TEA was added, melting of E1:12345 was not reversible with 0.060 M $MgCl_2$ present. Nevertheless, TEA addition in the presence of 0.060 M $MgCl_2$ lowered the temperature of the melting response of E1:12345 (Figure 10B), as did TEA addition without Mg^{2+} present (Figure 10A).

CONCLUSION

The large apparent activation energy of SJH by E1:12345 (Figures 5 and 6B) implies that both changing the conformational state and occupying the transition state are increased by raising the temperature toward T_{max}. We propose that E1:12345 molecules are distributed among at least three states of conformational equilibrium: compact(C), open(O), and disordered(D). Each of these states, and also the transition

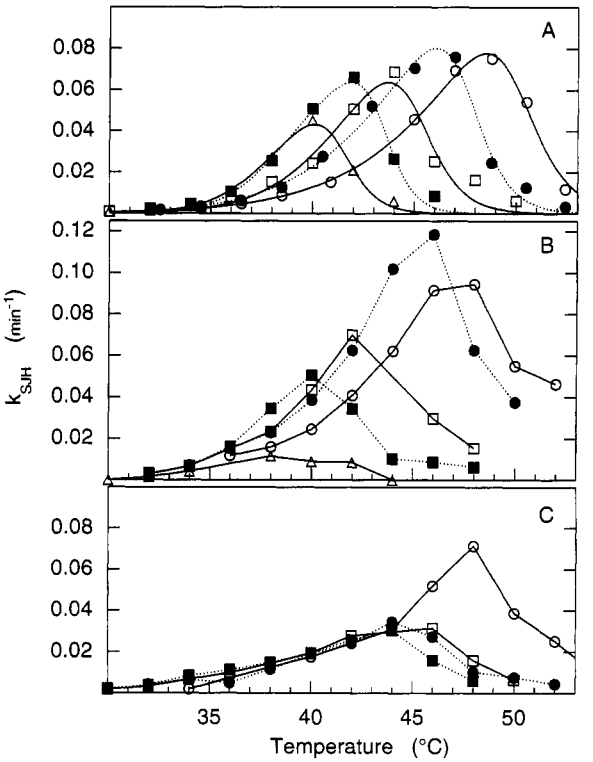

FIGURE 8: Effect of TEA and urea on the temperature response of the SJH rate. (A) 0.50 M KCl plus TEA at concentrations of (○) 0.0, (●) 0.20, (□) 0.40, (■) 0.80, and (△) 1.0, M. The rate constants were determined by method iii with 5-min reactions. The curves were drawn by fitting according to Appendix eq 6a, and the pertinent parameter values are listed in Table 3. (B) 1.0 M KCl plus TEA at concentrations of (○) 0.0, (●) 0.20, (□) 0.40, (■) 0.60, and (△) 0.80 M, with method iii reaction times ranging from 2.5 min at T_{max} to 20 min at 28 °C in 0.80 M TEA. (C) 0.50 M KCl plus urea at concentrations of (○) 0.0, (●) 0.50, (□) 0.75, and (■) 1.0 M, with varying method iii reaction times.

state, may comprise a set of substates over which any state function is averaged; therefore changes in thermodynamic variables such as $\Delta H^{\ddagger}$ represent differences between the average values of the final and initial sets of substates. The states C, O, and D are represented in Scheme 2, where K_{CO} and K_{OD} are the equilibrium constants for the conformational transitions C → O and O → D, respectively.

The equilibrium constants in Scheme 2 are presumed to be temperature dependent in the usual way (as elaborated in eq 6a of the Appendix). The three-state model holds that

Table 3: SJH Reaction Parameters According to the Three-State and Two-State Models

parameter	[TEA] (M) 0.0[a]	0.0[b]	0.2[b]	0.4[b]	0.5[a]	0.8[b]	1.0[b]
$\Delta H^{\ddagger}$ (kcal mol^{-1})	22.6 (three-state) 50.5 (two-state)	[c]	[c]	[c]	[c] (three-state) 54.1 (two-state)	[c]	[c]
$\Delta S^{\ddagger}$ (eu)	0 (three-state) 86 (two-state)	[c]	[c]	[c]	[c] (three-state) 99.2 (two-state)	[c]	[c]
$\Delta H°_{CO}$ (kcal mol^{-1})	44 (three-state) na[d] (two-state)	40	56	85	86 (three-state) na (two-state)	130	117
$\Delta S°_{CO}$ (eu)	138 (three-state) na (two-state)	124	178	272	277 (three-state) na (two-state)	417	376
$T_{0.5,CO}$ (°C)	45.9 (three-state) na (two-state)	46.6	41.7	40.2	38.9 (three-state) na (two-state	37.9	37.3
$\Delta H°_{OD}$ (kcal mol^{-1})	175 (three-state) 223 (two-state)	194	229	217	208 (three-state) 184 (two-state)	285	252
$\Delta S°_{OD}$ (eu)	545 (three-state) 793 (two-state)	601	714	682	652 (three-state) 580 (two-state)	900	800
$T_{0.5,OD}$ (°C)	48.3 (three-state) 48.8 (two-state)	49.5	47.4	45.0	45.4 (three-state) 44.6 (two-state)	43.4	41.3

[a] Rate constants were determined by Method ii. [b] Rate constants were determined by Method iii. [c] The three-state model was applied to these data, using the three-state $\Delta H^{\ddagger}$ and $\Delta S^{\ddagger}$ values from the second column of this table. [d] na: Not applicable to the two-state analysis.

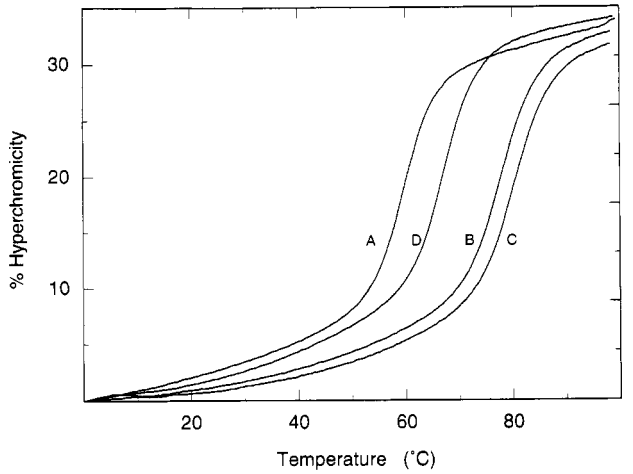

FIGURE 9: Effect of TEA on the hyperchromicity–temperature profiles of GGD5. All solutions contained the reference buffer 0.020 M cacodylate at pH 7.0 plus 0.0005 M EDTA. The added components for each melting were as follows: (A) no additions, (B) 0.5 M KCl, (C) 1.0 M KCl, and (D) 0.5 M KCl plus 0.5 M TEA. The curves were drawn according to the two-state model using the appropriate thermodynamic parameter values from Table 2 and the appropriate limiting-line parameter values derived by a standard method (Petersheim & Turner, 1983).

E1:12345 is predominantly in a compact (SJH-incompetent but folded) conformation at low temperatures, that E1:12345 is converted to an open (folded but reactive) conformation as the temperature is raised, and that E1:12345 finally reaches a disordered (at least partly unfolded and inactive) state at still higher temperatures. A two-state model with open and disordered states can be derived from Scheme 2 simply by asserting that K_{CO} is very large (see eqs 7 and 7a). Such a two-state formulation dictates a specific response to the addition of compounds that disrupt RNA structure. Such agents act by increasing K_{OD}, while exerting little or no effect on the intrinsic rate of phosphodiester bond cleavage. This means that the $\Delta H^{\ddagger}$ and $\Delta S^{\ddagger}$ values for the cleavage chemistry *per se* should hardly change upon addition of the structure-breaking agent. Significantly, k_{SJH} is expected to decrease at all temperatures in the two-state model (see eq 7a).

The data of Figure 6B are not consistent with such a two-state model. Fitting these data to the two-state model requires adjusting the $\Delta H^{\ddagger}$ and $\Delta S^{\ddagger}$ values for the reactions with TEA (see columns 2 and 6 of Table 3). Moreover, the $\Delta H^{\ddagger}$ and $\Delta S^{\ddagger}$ values required for these fits are inordinately large compared to the data for the reference phosphodiester (or monoester) bond cleavages shown in Table 1. However, fitting the 0.5 M TEA k_{SJH} values of Figure 6B, while maintaining $\Delta H^{\ddagger}$ and $\Delta S^{\ddagger}$ constant, is readily achieved with the three-state model (eq 6a). Because of the complexity of the equation, analysis of the data of Figure 6B according to this three-state model required us to make an arbitrary, but not unreasonable, initial choice. We fixed the value of $\Delta S^{\ddagger}$ at 0, a value within the range of values in Table 1. Interestingly, the value of $\Delta H^{\ddagger}$ (22.6 kcal mol^{-1}) obtained by fitting with this choice for $\Delta S^{\ddagger}$ is within the range of the Table 1 entries. Keeping $\Delta H^{\ddagger}$ and $\Delta S^{\ddagger}$ constant at these values, in accord with the constraints of the three-state model, allowed satisfactory matching of the calculated response to the data obtained in the presence of 0.50 M TEA. Using the same values of $\Delta H^{\ddagger}$ and $\Delta S^{\ddagger}$, we also fitted the broader span of data obtained by method iii (Figure 8A). The resulting parameters characterize the C → O and O → D transitions over the range of 0.0–1.0 M TEA (Table 3). The use of $\Delta S^{\ddagger}$ values both larger and smaller than zero resulted in poorer fits to the three-state formulation (see Materials and Methods). However, though the fit was poorer with these choices for $\Delta S^{\ddagger}$, the derived $\Delta H°$ and $\Delta S°$ values for the C → O and O → D transitions were still increased by added TEA. In contrast, the two-state model simply cannot fit these data if $\Delta H^{\ddagger}$ and $\Delta S^{\ddagger}$ are held constant.

Using the $\Delta H°$ and $\Delta S°$ values from Table 3 for the C → O and O → D transitions, one can calculate the distribution of the C, O, and D conformers as they vary with temperature for the TEA concentrations examined (see eqs 8a–8c). Figure 11 shows the fraction of RNA present as the open (SJH active) form. TEA enhances both the C → O and O → D transitions at any given temperature and thereby shifts the distribution of SJH-active forms to lower temperatures. This shift in the temperature-dependent distribution of SJH-active forms of E1:12345, along with the conventional heat-dependent populating of the reaction transition state, accounts for the observed variation of k_{SJH} with temperature.

According to the entries of Table 3, the action of TEA to lower the C → O and O → D transition midpoint temperatures appears to be entropically driven. Such an entropy-promoted destabilization of RNA secondary structure by TEA is also seen with GGD5 melting in the presence of KCl (Table 2). Whereas increasing the concentration of KCl from 0.50 to 1.0 M stabilized GGD5 ($\Delta T_m \approx 2$ °C) by lowering the entropy of melting, adding an equivalent amount of TEA to the 0.50 M

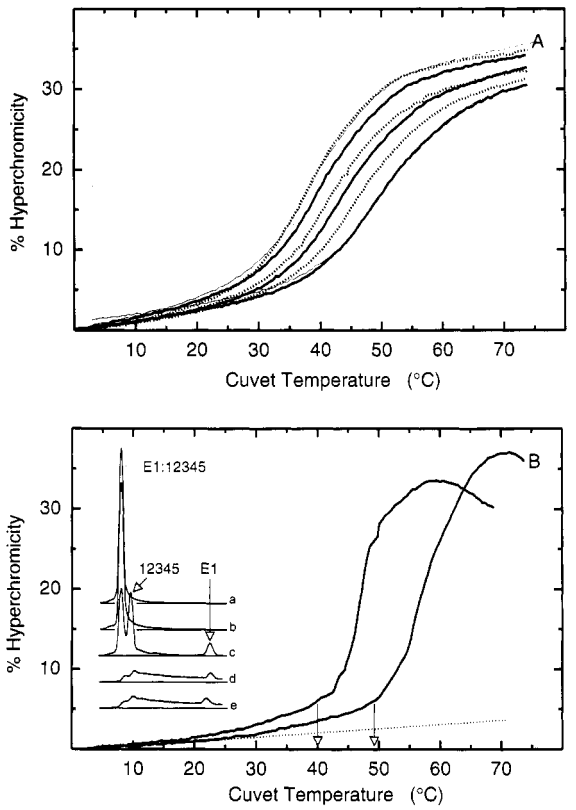

FIGURE 10: Effect of TEA on the hyperchromicity *versus* temperature response of E1:12345. E1:12345 was melted in the absence (A) and presence (B) of $MgCl_2$. (A) All cuvette solutions contained 0.50 M KCl, 0.020 M HEPES (pH 7.1), and 0.0005 M EDTA. From right to left, the alternating solid and dotted melting profiles represent the following concentrations of TEA: 0.0, 0.20, 0.40, 0.60, 0.80, and 1.0 M. The very thin profile curves closely adjacent to the 0.0 and 1.0 M TEA profiles are the cooling portions of those heating-and-cooling cycles. Similar cooling curves at the intermediate TEA concentrations are not shown. (B) E1:12345 was melted in 0.50 M KCl, 0.020 M HEPES (pH 7.1), and 0.060 M $MgCl_2$. The melting profile on the right represents no added TEA; the profile on the left represents 1.0 M TEA. The vertical arrows pointing to the abscissa indicate T_{max} for SJH under each of these conditions. The unframed inset on the left is the collection of AMBIS tracings of radioactivity *versus* migration distance in a 4% polyacrylamide gel for samples treated as follows: (a) the initial sample of E1:12345, (b) the sample after undergoing heating and cooling in the cuvette (0 to 75 to 0 °C over 80 min) in the standard SJH reaction buffer but without added $MgCl_2$, (c) a sample treated like sample b and then incubated for 12 min at 48 °C with the addition of 0.060 M $MgCl_2$, (d) a sample in the presence of 0.060 M $MgCl_2$ after undergoing heating and rapid chilling in the cuvette, and (e) a sample treated like sample d after subsequent incubation for 12 min at 48 °C.

Scheme 2

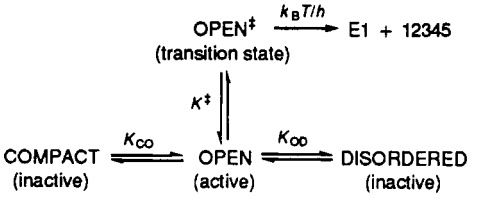

KCl solution destabilized GGD5 ($\Delta T_m \approx -11$ °C) by raising the entropy of melting. This action of TEA—to destabilize RNA structure by differentially increasing the enthalpy and entropy of unfolding processes—may be rationalized in terms of preferential solvation effects (see section C of the Appendix).

TEA cations not only serve as counterions but also interact directly with DNA bases both in double-stranded regions (Shapiro et al., 1969) and, preferentially, in single-stranded regions (Melchior & von Hippel, 1973). Our results indicate that TEA acts similarly on RNA. Direct interaction of TEA

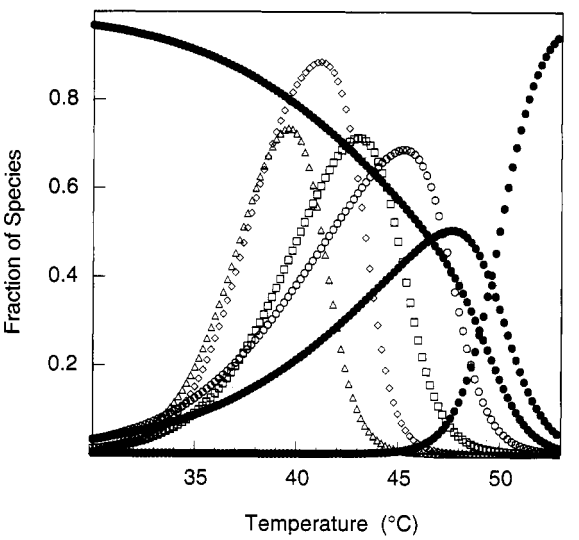

FIGURE 11: Population distributions of the conformational states of the three-state model as a function of temperature. The fractional amounts of each species were calculated using Appendix eqs 8a–c with the appropriate parameter values from Table 3. In 0.50 M KCl with no TEA present (●), the decreasing response, the intervening peaking function, and the increasing response with increasing temperature represent, respectively, the fractions of compact, open and disordered three-state model forms of E1:12345. In the presence of TEA at concentrations of (○) 0.20, (□) 0.40, (◇) 0.80, and (△) 1.0 M, only the distribution of the open form population is shown.

cations with the nucleotide bases presumably displaces some water of hydration from RNA. The number of water molecules thus displaced is likely to exceed the number of TEA cations bound, since a TEA cation is much larger than one water molecule. Likewise, the binding of TEA to RNA must result in the release of some of the structured water surrounding the TEA cations (Frank & Wen, 1957). Evidently, these two modes of water liberation act together and more than compensate for the oppositely acting entropic effect of anchoring TEA preferentially onto the unfolded RNA. The positive values of the $\Delta(\Delta H°_{CO})$ and $\Delta(\Delta S°_{CO})$ parameters are consistent with this picture; that is, RNA·TEA interactions are accompanied by a net release of water from hydrated RNA and structured water–TEA. Thus, the effect of TEA to enhance SJH by E1:12345 at temperatures below T_{max} is entropy driven.

Some other models are not inconsistent with the observations described here. For example, one can formulate a scheme involving two states in equilibrium, ordered and disordered, molecules of the former state undergoing sequentially the steps of conformational rearrangement and specific SJH. On the premise that the second step, chemistry, is insensitive to TEA, one can deduce that the preceding step, conformational change, is rate limiting. According to a variation of this scheme, the ordered state directly yields the specific SJH products in a single step that comprises both conformational and chemical elements. Essentially, this is our two-state model, modified to accommodate the observed large activation parameter values and TEA effects. Both of these models presuppose the involvement of significant conformational effects in the SJH process.

In summary, two independent findings have been presented here that are not consistent with the simple two-state model, but both can be readily accommodated with the three-state model. The first is the magnitude of $\Delta H^‡_{app}$, along with that of $\Delta S^‡_{app}$, which are unreasonably large for just the chemical step. The second is the nature of the TEA-induced shift of the SJH rate *versus* temperature profile. The values of the characterizing parameters governing this shift imply that TEA

reduces the stability of folded RNA through an entropically favorable release of bound water. One corollary of the three-state model is that the folded structure of isolated group II introns with the lowest free energy is unlikely to represent the active conformation of these complex ribozymes. Finally, it seems likely that the open conformation identified by this work represents only one of the active conformations available to self-splicing group II introns, since lariat formation and the second step of splicing were specifically prevented by our choice of experimental transcript.

ACKNOWLEDGMENT

The authors thank Professor C. Robert Matthews of the Chemistry Department at Pennsylvania State University for the use of his Aviv 14DS spectrophotometer equipped with a thermoelectric temperature-regulated sample holder. This instrument was used in our initial melting studies. We thank Dr. Philip S. Perlman of the University of Texas at Dallas for supplying plasmid pJD-I3′-851, for his continued interest in this project, and for communicating unpublished results. We also thank Professor James M. Pipas of our own department for critically reviewing a preliminary manuscript and suggesting significant editorial improvements.

APPENDIX

(A) Rate Equations for E1:12345 SJH. The reaction model of Scheme 1 leads to the progress functions defined by eqs 1–3, following the usual approaches for analyzing consecutive and parallel processes (Frost & Pearson, 1953).

$$\frac{[B]}{[A]_0} = \frac{k_{SJH}}{k_{SJH} + k_{rs}^A}(1 - e^{-(k_{SJH} + k_{rs}^A)t}) \quad (1)$$

$$\frac{[B]}{[A]_0} = k_{SJH}t \quad (1a)$$

$$\frac{[C]}{[A]_0} = \frac{k_{SJH}}{k_{SJH} + k_{rs}^A - (k_{\psi SJH} + k_s^C)}(e^{-(k_{\psi SJH} + k_{rs}^C)t} - e^{-(k_{SJH} + k_{rs}^A)t}) \quad (2)$$

$$\frac{[D]}{[A]_0} = \frac{k_{SJH}\,k_{\psi SJH}}{k_{SJH} + k_{rs}^A - (k_{\psi SJH} + k_{rs}^C)}\left\{\frac{1}{k_{\psi SJH} + k_{rs}^C}[1 - e^{-(k_{\psi SJH} + k_{rs}^C)t}] - \frac{1}{k_{SJH} + k_{rs}^A}[1 - e^{-(k_{SJH} + k_{rs}^A)t}]\right\} \quad (3)$$

At short times, the linear period of reaction, eq 1 reduces to eq 1a. The inclusion of decay processes for species B and D of Scheme 1, governed by rate constants k_{rs}^B and k_{rs}^D, may be formally included in a straightforward manner and result in modified versions of eqs 1 and 3, respectively. Formal inclusion of the effect of random scission of B yielded negligibly small values of k_{rs}^B; loss of B by this mode was inconsequential. The data for the appearance of D extended only over its formation phase, and the amount of D produced was relatively small. Therefore, k_{rs}^D could not be reliably evaluated and was also set to zero, as is implicit in eq 3.

(B) Temperature Dependence of the SJH Rate Constant in Terms of Two-State and Three-State Systems. The mass balance relation for the RNA system of Scheme 2 at time zero of any SJH reaction is given by eq 4:

$$RNA_{total} = C + O + O^{\ddagger} + D \approx C + O + D \quad (4)$$

k_{SJH} for this three-state system can readily be written as eq 5:

$$k_{SJH} = (k_B T/h)\frac{K^{\ddagger}[O]}{[RNA_{total}]} \quad (5)$$

By applying the mass balance relation and the definitions for the equilibrium constants K_{CO} and K_{OD}, eq 5 becomes eq 6.

$$k_{SJH} = \frac{\frac{k_B T}{h}K^{\ddagger}K_{CO}}{1 + K_{CO}(1 + K_{OD})} \quad (6)$$

Alternatively, this relation may be expressed as eq 6a, where T_{CO} and T_{OD} are the midpoint temperatures for the C → O and O → D transitions, respectively. The corresponding $\Delta S°$ values are obtained as $\Delta H°_{CO}/T_{CO}$ and $\Delta H°_{OD}/T_{OD}$.

$$k_{SJH} = \frac{\frac{k_B T}{h}e^{\Delta S^{\ddagger}/R}e^{-\Delta H^{\ddagger}/RT}e^{-(\Delta H°_{CO}/R)((1/T) - (1/T_{CO}))}}{1 + e^{-(\Delta H°_{CO}/R)((1/T) - (1/T_{CO}))}(1 + e^{-(\Delta H°_{OD}/R)((1/T) - (1/T_{OD}))})} \quad (6a)$$

A simpler two-state description of E1:12345, with only states O and D, is obtained by asserting that K_{CO} is much greater than 1. Eq 6 then reduces to eq 7.

$$k_{SJH} = \frac{\frac{k_B T}{h}K^{\ddagger}}{1 + K_{OD}} \quad (7)$$

Equation 7 in turn may be alternatively expressed as

$$k_{SJH} = \frac{\frac{k_B T}{h}e^{\Delta S^{\ddagger}/R}e^{-\Delta H^{\ddagger}/RT}}{1 + e^{-(\Delta H°_{OD}/R)((1/T) - (1/T_{OD}))}} \quad (7a)$$

The relative populations of the conformational forms C, O, and D of the three-state system may be obtained by relations 8a–c:

$$\frac{[C]}{[A]_0} = \frac{1}{1 + K_{CO}(1 + K_{OD})} \quad (8a)$$

$$\frac{[O]}{[A]_0} = \frac{K_{CO}}{1 + K_{CO}(1 + K_{OD})} \quad (8b)$$

$$\frac{[D]}{[A]_0} = \frac{K_{CO}K_{OD}}{1 + K_{CO}(1 + K_{OD})} \quad (8c)$$

(C) Solvation and the Thermodynamics of RNA Unfolding. The following chemical equations, where F and U represent more and less folded states of RNA, illustrate the solvation changes pertinent to RNA unfolding promoted in the absence, eq 9a, and in the presence, eq 9b, of TEA:

$$F{\cdot}(H_2O)_i = U{\cdot}(H_2O)_j + (i - j)H_2O \quad (9a)$$

$$(n - m)TEA{\cdot}(H_2O)_p + F{\cdot}(H_2O)_k{\cdot}(TEA)_m = U{\cdot}(H_2O)_l{\cdot}[(TEA)_n{\cdot}(H_2O)_q] + (k - l)H_2O + (p - q)(n - m)H_2O \quad (9b)$$

The solvation numbers of F and U are presumably subject to the following inequalities:

$(i > j)$	If DNA is an appropriate model for RNA hydration, folded RNA is more hydrated by 2 or 3 waters per base pair than unfolded RNA (Chapman & Sturtevant, 1969).
$(i > k)$ and $(j > l)$	TEA binding displaces water.
$(n > m)$ and $(k > l)$	TEA prefers unfolded RNA (Melchior & von Hippel, 1973).
$(i - k > m)$ and $(j - l > n)$	Each TEA binding releases more than one water because of steric displacement.

The unfolding enthalpy and entropy, $\Delta H°_{FU}$ and $\Delta S°_{FU}$, in the absence and presence of TEA, can be written as sums of their contributing terms as shown in eqs 10a–d.

$$\Delta H°_{FU}^{-TEA} = \Delta H°_{\text{unfolding}} + (i-j)\Delta h_{H_2O \text{ release from RNA}} \quad (10a)$$

$$\Delta S°_{FU}^{-TEA} = \Delta S°_{\text{unfolding}} + (i-j)\Delta s_{H_2O \text{ release from RNA}} \quad (10b)$$

$$\Delta H°_{FU}^{+TEA} = \Delta H°_{\text{unfolding}} + (k-l)\Delta h_{H_2O \text{ release from RNA}} + (p-q)(n-m)\Delta h_{H_2O \text{ release from TEA}} + (n-m)\Delta h_{\text{TEA binding}} \quad (10c)$$

$$\Delta S°_{FU}^{+TEA} = \Delta S°_{\text{unfolding}} + (k-l)\Delta s_{H_2O \text{ release from RNA}} + (p-q)(n-m)\Delta s_{H_2O \text{ release from TEA}} + (n-m)\Delta s_{\text{TEA binding}} \quad (10d)$$

The incremental changes, $\Delta(\Delta H°)$ and $\Delta(\Delta S°)$, in the apparent unfolding enthalpies and entropies due to TEA addition are now observed to result solely from solvation effects as demonstrated by eqs 11a,b.

$$\Delta(\Delta H°) = [(k-l)-(i-j)]\Delta h_{H_2O \text{ release from RNA}} + (p-q)(n-m)\Delta h_{H_2O \text{ release from TEA}} + (n-m)\Delta h_{\text{TEA binding}} \quad (11a)$$

$$\Delta(\Delta S°) = [(k-l)-(i-j)]\Delta s_{H_2O \text{ release from RNA}} + (p-q)(n-m)\Delta s_{H_2O \text{ release from TEA}} + (n-m)\Delta s_{\text{TEA binding}} \quad (11b)$$

REFERENCES

Altman, S., & Guerrier-Takada, C. (1986) *Biochemistry 25*, 1205–1208.

Brown, D. M., & Usher, D. A. (1965) *J. Chem. Soc. (London)*, 6558–6564.

Bunton, C. A., Llewellyn, D. R., Oldham, K. G., & Vernon, C.A. (1958) *J. Chem. Soc. (London)*, 3574–3587.

Bunton, C. A., Mhala, M. M., Oldham, K. G., & Vernon, C. A. (1960) *J. Chem. Soc. (London)*, 3293–3301.

Celander, D. W., & Cech, T. R. (1991) *Science 251*, 401–407.

Chang, C.-T., Hain, T. C., Hutton, J. R., & Wetmur, J. G. (1974) *Biopolymers 13*, 1847–1858.

Chapman, R.E., Jr., & Sturtevant, J. M. (1969) *Biopolymers 7*, 527–537.

Ferat, J.-L., & Michel, F. (1993) *Nature*, 358–361.

Frank, H. S., & Wen,W.-Y. (1957) *Discuss. Faraday Soc. 24*, 133–140.

Franzen, J. S., Zhang, M., & Peebles, C. L. (1993) *Nucleic Acids Res. 21*, 627–634.

Frost, A. A., & Pearson, R. G. (1953) *Kinetics and Mechanism*, pp 153–154, John Wiley & Sons, Inc., New York.

Grosshans, C. A., & Cech, T. R. (1989) *Biochemistry 28*, 6888–6894.

Hawkins, E. R., Chang, S. H., & Mattice, W. L. (1977) *Biopolymers 16*, 1557–1566.

Herschlag, D., & Cech, T. R. (1990) *Biochemistry 29*, 10159–10171.

Jarrell, K. A., Peebles, C. L., Dietrich, R. C., Romiti, S. L., & Perlman, P. S. (1988) *J. Biol. Chem. 263*, 3432–3439.

Koch, J. L., Boulanger, S. C., Dib-Hajj, S. D., Hebbar, S. K., & Perlman, P. S. (1992) *Mol. Cell. Biol. 12*, 1950–1958.

Kück, U., Godehart, I., & Schmidt, U. (1990) *Nucleic Acids Res. 18*, 2691–2697.

Kumomoto, J., Cox, J. R., Jr., & Westheimer, F. H. (1956) *J. Am. Chem. Soc. 78*, 4858–4860.

Melchior, W.B., Jr., & von Hippel, P. H. (1973) *Proc. Natl. Acad. Sci. U.S.A. 70*, 298–302.

Michel, F., Umesono, K., & Ozeki, H. (1989) *Gene 82*, 5–30.

Milligan, J. F., & Uhlenbeck, O.C. (1989) *Methods Enzymol. 180*, 51–62.

Moore, M. J., Query, C. C., & Sharp, P.A. (1993) in *The RNA World* (Gesteland, R. F., & Atkins, J. F., Eds.) pp 303–357, Cold Spring Harbor Laboratory Press, Cold Spring Harbor, New York.

Peebles, C. L., Perlman, P. S., Mecklenburg, K. L., Petrillo, M. L., Tabor, J. H., Jarrell, K. A., & Cheng, H. L. (1986) *Cell 44*, 213–223.

Peebles, C. L., Benatan, E. J., Jarrell, K. A., & Perlman, P. S. (1987) *Cold Spring Harbor Symp. Quant. Biol. 52*, 223–232.

Petersheim, M., & Turner, D.H. (1983) *Biochemistry 22*, 256–263.

Piccirilli, J. A., Vyle, J. S., Caruthers, M. H., & Cech, T. R. (1993) *Nature 361*, 85–88.

Schleich, T., & Gould, G. R. (1974) *Biopolymers 13*, 327–337.

Shapiro, J. T., Stannard, B. S., & Felsenfeld, G. (1969) *Biochemistry 8*, 3233–3241.

Simha, R. (1941) *J. Appl. Phys. 12*, 569–578.

Shub, D. A., Peebles, C. L., & Hampel, A. (1994) in *RNA Processing: A Practical Approach* (Higgins, S. J., & Hames, B. D., Eds.) Vol. II, pp 211–239, IRL Press, Oxford.

Smith, D. R., & Pace, N. R. (1993) *Biochemistry 32*, 5273–5281.

Steitz, T. A., & Steitz, J. A. (1993) *Proc. Natl. Acad. Sci. U.S.A. 90*, 6498–6502.

Sugimoto, N., Kierzek, R., & Turner, D.H. (1988) *Biochemistry 27*, 6384–6392.

Tanford, C. (1961) *Physical Chemistry of Macromolecules*, pp 615–616, John Wiley & Sons, Inc., New York.

von Hippel, P. H., & Schleich, T. (1969) in *Biological Macromolecules* (Fasman, G., & Timasheff, S., Eds.) Vol. 2, pp 417–574, Marcel Dekker, New York.

Walstrum, S. A., & Uhlenbeck, O. C. (1990) *Biochemistry 29*, 10573–10576.